

SSC99-V-6

Free Flying Magnetometers As a Demonstration of Micro-spacecraft Technologies

J. Willis, K. Leschly, H. Javadi, B. Blaes, K. Boykins
Jet Propulsion Laboratory
4800 Oak Grove Dr.
Pasadena Ca 91109

D. Rau
University of New Hampshire
Durham, NH

Abstract. Four Free Flying Magnetometers (FFMs) flew on the Enstrophy sounding rocket launched on February 10, 1999 from Poker Flats Research Range. Each of these FFMs is a highly integrated “sensorcraft”, containing their own data, attitude determination, telecom, and power systems in addition to a small 3-axis magnetometer. All of this was fit into a package a little bigger than a hockey puck and weighed less than 250 grams. The FFM technology development task was funded by NASA/JPL.

INTRODUCTION

The Enstrophy mission was proposed jointly by the University of New Hampshire, Cornell University, and JPL to NASA in response to the Space Physics NRA of 1996 (PI: Prof. Kristina Lynch). Its goal was to make multiple-point measurements of the magnetic field in the northern auroral zone via four small free flying sensorcrafts. The results of these measurements have been used to calculate magnetic-field-aligned current density along the rocket trajectory. The mission technical objective was the proof of concept of the JPL FFM design. The scientific goal was to study the structure of small-scale current systems in the night side auroral region.

This paper will describe the realization of the first FFM sensorcraft as intended for a specific NASA mission. Details related to the Enstrophy mission and its scientific achievements will be reported in the future [1-3].

DESIGN

The Free-Flying Magnetometer sensorcraft was designed for the specific needs of the Enstrophy mission. Each of the FFMs contained a miniaturized 3-axis 1 nanoTesla (nT) fluxgate magnetometer that was sampled at ~70 Hz. Additionally the FFMs were

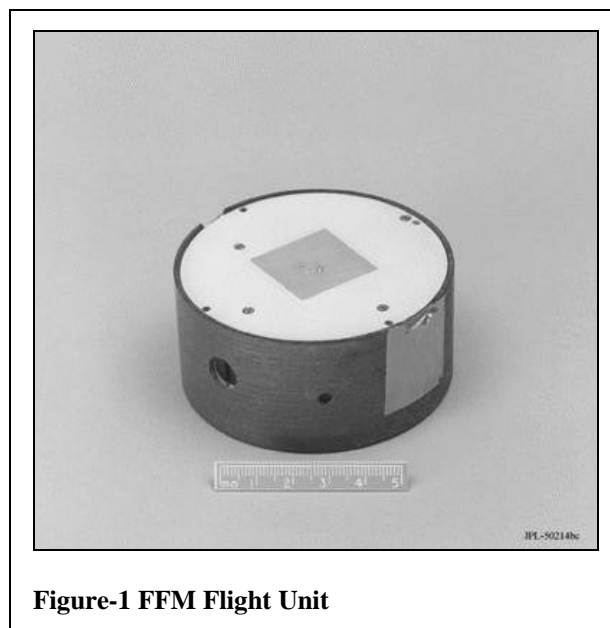


Figure-1 FFM Flight Unit

designed to minimize magnetic signature and its effect on the magnetometer. The FFMs design allowed the precise measurements of the magnetic field along the FFM flight path required to determine the current density that was the goal of the Enstrophy mission.

Each of the FFMs contained the fluxgate magnetometer, integrated data & power

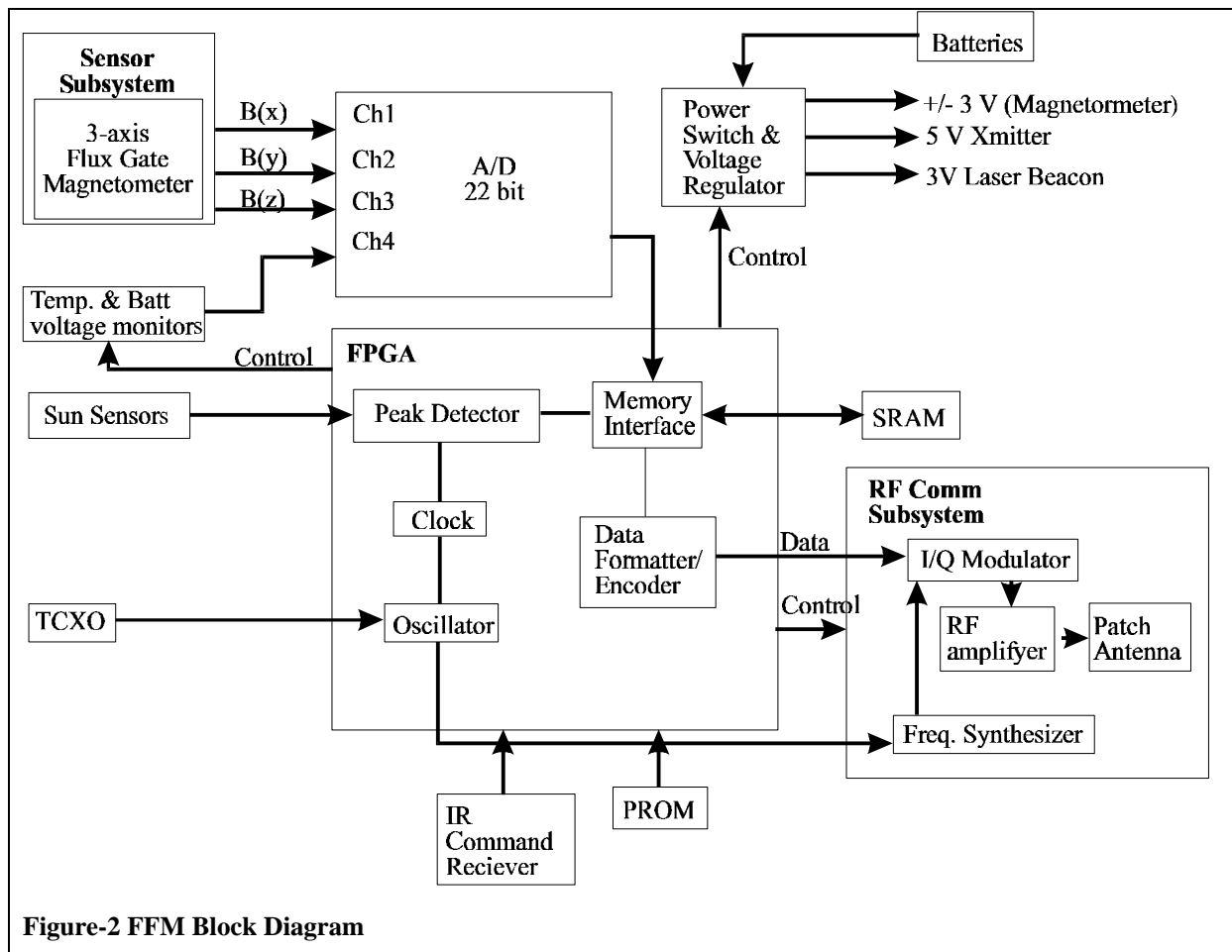


Figure-2 FFM Block Diagram

system, two sun sensors, a laser beacon, Lithium Chloride batteries and an S-band transmitter. This section will describe the FFM design in detail, how they were mechanically integrated and the release mechanism.

FFM Integrated Data Subsystem

The FFM data subsystem design encompassed both analog and digital electronics as well as power regulation and management. The FFM data subsystem was centered around a Field Programmable Gate Array (FPGA) that controlled all of the functions of the FFM. The FPGA used for the FFM was a 13000-gate count chip in a plastic package (Xilinx, XC4013-E). This FPGA sampled the digital sun sensors and analog to digital converter (ADC), controlled the power system, and formatted and encoded the data packets that were sent by the RF subsystem. A block diagram of the data system is shown in Figure-2.

The ADC that was used in the FFM was a high resolution 22-bit 4-channel ADC that was sampled at 70Hz. Channels 1-3 of the ADC were connected to the magnetometer X, Y, and Z outputs. Channel 4 was connected to a multiplexer connected to eight engineering data sensors. Four of these sensors were temperature sensors. The temperature sensors were mounted on the magnetometer core, magnetometer PCB, the TCXO, and the fourth was mounted on the analog board in the vicinity of the ADC. There were four other sensors that monitored three supply voltages and a voltage baseline.

The data from sun sensors and the ADC was stored in a 4 Mbit SRAM that stored the 2547 frames of data generated during each data acquisition/transmission cycle. Each frame contained a frame ID, time tag, FFM unique ID, sun sensor data, engineering sensor data, and the most significant 17-bits of data from channels 1-3 of the ADC.

Power for the FFM was supplied by 4 high-capacity LiSOCl₂ batteries that supported

more than 1.5 hours life span for a FFM unit. Typical dimensions of the LTC-312 (Eagle Picher Industries, Inc. [7]) battery were 2.5 x 17.5 x 37.1 mm. These batteries were chosen for their long shelf life (~3% degradation/year) and high energy density. The voltages from the batteries were regulated by linear regulators to the voltages required by each of the subsystems. The power was controlled by the FPGA via solid state switches.

FFM Miniaturized Fluxgate Magnetometer

A miniaturized 3-axis high field fluxgate magnetometer was developed for the FFM. The magnetometer consisted of one toroidal core (with coil windings for X and Y axes) and one racetrack shaped core placed in the middle of the toroidal one (with single coil winding along the Z-axis). The cores were made out of a compound with superior noise properties. Drive electronics for the cores and the read-out electronics were implemented on two PCBs (Figure 5). Commercial off-the-shelf electronic components were used.

Applied Physics Systems (Mountain View, CA) under a contract from JPL developed this miniaturized 3-axis fluxgate magnetometer with the characteristics found in Table 1.

Temperature dependence of the magnetometer drift and scale factor was of concern. A thermal analysis of near-final FFM package was done. We assumed Earth IR heating on the FFM antenna and the FFM shell cylindrical

side with the opposite endplate looking into cold sky. The calculations showed that near final thermal configuration with the magnetometer top PCB thermally isolated from the core (starting at initial temperature of 25° C) and counting power dissipations of the FFM subsystems, the thermal gradient across the top PCB is less than ~4° C reducing to ~2° C when magnetometer top PCB is thermally connected to the core.

One of the biggest challenges of the FFM project was integration of live electronics in close vicinity of a sensitive magnetometer. Our goal was to limit total DC interference of the electronics and packaging materials on the magnetometer to <1 nT. All electronics components were screened for low magnetic signature. We avoided ceramic packages with Kovar leads, most RF connectors and semirigid cables, and large capacitors containing Ni in their metal electrodes. Non-magnetic A-286 steel was used in construction of the sun-sensor body. All electronic components were degaussed before soldering onto the boards. The electronic boards were also degaussed before final assembly. DC magnetic fields of major current carrying traces on the FFM digital and analog boards were calculated at position of the magnetometer core. Careful routing of traces was made to minimize the interference. Calculations showed that the overall effect must be below 1 nT. In principle, constant DC magnetic field generated by the current traces in the layout can be calibrated out and its effect is

- Maximum signal:	+/- 60,000 nT
-Orthogonality range (typical):	1 - 3 degree (+-0.5 degree error)
- Sensitivity:	2.0 V / 60000 nT
-Magnetic noise level (typical):	<0.06nT rms/sqrt(Hz) at 1 Hz, 1/f below 1 Hz
-Frequency response (typical):	DC to 100 Hz (3 dB)
- Linearity:	<0.1% FS
-Temperature coefficient:	Strong temperature dependencies (is modified with proper thermal packaging)
- Drift (typical):	< 20 nT / 20 min. < 2 nT/1 min. < ~0.3 nT/1 sec.
-Power consumption (typical):	+3V @ 60 mA -3V @ 60 mA
- Size (cylindrical):	38 mm diameter x 17 mm long
- Packaging: thermal design: mechanical design:	extended ground plane PCBs, upper PCB is thermally connected to the magnetometer cores. provides coordinate references

minimized when measurements of magnetic field variations are of interest.

A typical FFM magnetometer noise power spectrum (while integrated with the FFM analog and digital boards but prior to integration with the FFM transmitter and batteries) was measured to be approximately $0.2/f + 0.02 \text{ nT}^2 / \text{Hz}$. This corresponds to a standard deviation of $\sim 1.2 \text{ nT}$ over the frequency band of interest. Detailed FFM magnetometer noise data will be reported in future publications.

FFM IR Command Receiver

External control of the FFM was accomplished through an IR command receiver that received IR signals not unlike those used in a TV remote control from either the Enstrophy payload or FFM GSE. Commands to power on or off the FFMs and to enter into the test or flight modes were communicated to each FFM through this interface. This interface scheme was chosen to minimize the complexity of the FFM release mechanism, as there are no wires to cut during release. One drawback of this design is that the receiver is always consuming power, ($< 30 \mu\text{A}$ from 7 Volt battery) which limits the FFM shelf life once the battery is connected to ~ 1.5 months.

A total of 4 commands were distinguishable which were “Test”, “Power On”, “Flight”, “Power Off” in addition to a “Reset” pulse. The “Test” mode was used for nightly vertical test of FFMs while still inside the rocket. During this mode, each FFM measured about 100 frames of data and transmitted the data back to the main antenna at Poker Flat. This was accomplished via a pick-up antenna inside the rocket that in turn carried the signal to another antenna at the skin of the rocket for transmission. Each FFM was automatically turned-off after the “Test” sequence but could have also been forced off at any time with the “Power Off” command. The FFM power was turned on right before lift-off of the rocket by the “Power On” command. At this point the FFMs transmitted carrier which was used to verify that the FFMs were powered. Approximately 100 seconds into the flight, the “Flight” command followed by a “Reset” pulse were sent to the FFMs. The “Reset” pulse zeroed the clocks onboard all the FFMs. The “Reset” pulse originated from the 1 pulse-per-second output of a GPS receiver. After the “Reset” pulse, the FFMs entered their data

acquisition/transmission cycle and were deployed from the payload (See Fig. 4).

FFM Transmitter & Antenna

The FFM transmitter was composed of a frequency synthesizer, modulator, and RF amplifier. The frequency synthesizer used the frequency reference provided by the FFMs TCXO produce the carrier frequency (2235-2275 MHz) that was sent to the I/Q modulator that produced the Bi-Phase Shift Key (BPSK) signal. This signal was sent to the two-stage amplifier and was amplified to more than 20 mW and fed to the antenna.

The single-patch antenna on a 2 mm thick substrate (TMM6.060 Rogers Corp.) was designed and built by MicroPulse, Inc. [6] for the FFM project. A stripline hybrid was used for the antenna feed that was implemented on a FR-4 substrate. Two probes connected the hybrid feed to appropriate locations on the patch.

FFM Sun Sensors

The FFM prototype sun sensor was designed and tested at the US Army Research Laboratory [8]. Flight units were manufactured at JPL using non-magnetic materials and metal coatings. The FFM sun sensor had overall dimensions of 15.0 x 15.0 x 5.0 mm and utilized a new design of an optical slit with an obstructive pillar, smoothly curved reflectors and light absorbing ridges, and a miniature silicon solar cell. The sensor acted as a voltage/current source under incident light and thus did not need external power. The geometry and construction of the sun sensor is patent pending by personnel of the U.S. Army Research Laboratory. Two sun sensors were integrated with each FFM unit. They were mounted on the cylindrical wall of the FFM 180° apart looking radially outward with one sun sensor tilted by 30°. Combination of two sun sensors provided additional information about the FFM angular motion.

FFM Laser Beacon

One of the biggest technical problems for the Enstrophy mission was that of determining FFM attitude at night. The sun-sensors provided a good solution when the sun was in view of FFMs. FFM attitude determination at night was facilitated by using a laser diode with line-generator optics on each FFM, and corresponding linear photon-multiplying

receivers on the rocket. This setup allowed the orientation of the FFM to the rocket to be determined.

The commercial laser on each FFM had an 85° fan shaped beam with the laser beam divergence of ~0.3 mrad. The 670 nm diode laser had <3 mW total power when powered with a 5V supply. Each receiver on the rocket had a field of view of ~60° in the rocket’s spin plane and ~10° in the perpendicular direction. A large area avalanche photodiode was used to detect the beam.

FFM Mechanical Packaging

Figure-3 depicts details of FFM packaging design. A shell was constructed out of graphite fiber composite material with openings for the sun sensors, laser beacon, and IR photodetector. The IR detector was mounted on the analog board viewing outward along the FFM spin axis. Two sun sensors and the laser beacon viewed radially outward. A single sided digital board was mounted directly on top of the analog board separated by spacers. The digital board sat on a ledge within the

graphite composite shell. It allowed passage of wires and coaxial cables through cuts in its edge. The magnetometer was placed in the middle of a lithographic material (“science cup”) and was glued directly on the top of the digital board. Cavities inside the “science cup” mechanically supported the sun sensors and the laser beacon. Also additional cavities housed TCXO box and three shielded compartments of the RF transmitter. Four batteries and four (4) wedges were tucked in between the “science cup” and the shell. Openings were allowed for the passage of all wires and coaxial cables. The final stages of the RF transmitter were placed near the top board of the magnetometer and under the antenna. The antenna was fastened to the “science cup” inserts from the top. A double-sided copper tape wrapped along the edges of the antenna joined the antenna to the inner walls of the graphite composite shell. It shielded internal RF circuitry and cables from antenna radiation spillover. The FFM flight units were vibrated to the flight acceptance levels at JPL prior to final delivery. Then FFM units were dynamically spin balanced and mass imbalances were corrected by added weights.

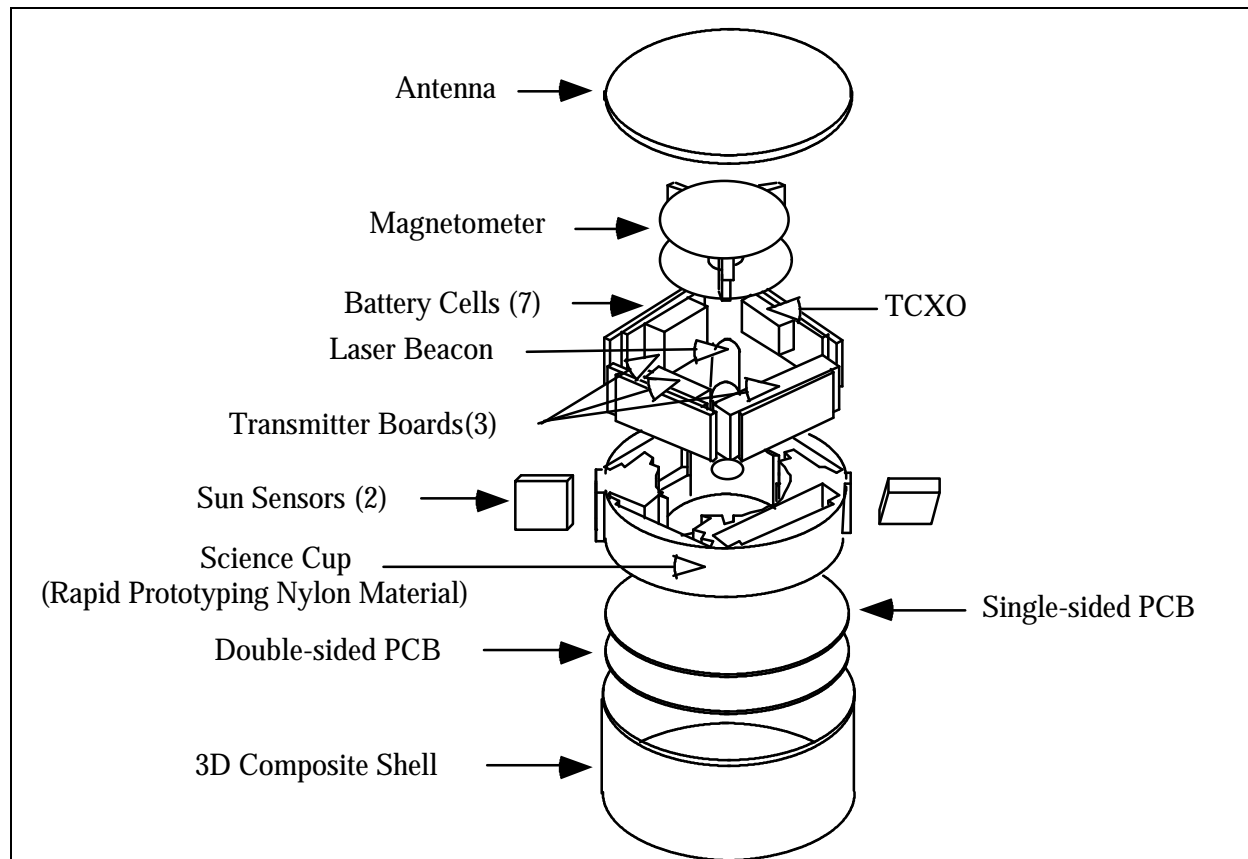


Figure-3 FFM Mechanical Configuration (Exploded View)

FFM Ejection Mechanism

Design of the ejection mechanism was based on roll (no slip) motion of each FFM within its individual spiral-shaped tract. The FFMs were originally held in the rocket with a spring-loaded stopper. Soon after the stopper was removed from the paths, the FFMs started rolling under the combined effect of coriolis and centrifugal force. As shown in Figure-4, two FFMs were stowed between two trays stacked perpendicular to the axis of the rocket and left the rocket exactly on the opposite ends of its diameter. The other two FFMs were kept right above them in separate trays with their exit openings rotated 90 degrees with respect to the lower trays.

THE MISSION

A three-stage Black Brant-10 sub-orbital rocket (Terrier, Black Brant - 5C, Nihka) was used in the Enstrophy Mission. The rocket was launched from the Poker Flat, Alaska range at about 10:45 PM local time on 2/10/99 (06:45 on 2/11/99 UTC) and reached altitude of 1070 km.

Table-2 describes the timeline of events for the FFMs during the Enstrophy Mission. Thirty seconds prior to launch the FFMs were turned on and set to flight mode by sending a command to the payload electronics which relayed the commands to the FFMs via their IR receivers. Nine seconds after launch these commands were automatically issued again by

the payload electronics incase the FFMs were reset during the first stage burn. Once the final stage had burnt out the FFMs were time synchronized using the onboard GPS receiver and were released 37 seconds later. At this point in the flight the payload was spinning at ~6 Hz and at an altitude of ~300 km. Once

Event	Time (sec)	Altitude (km)
FFM Flight Mode	-30.0	
Launch	0.0	
Terrier Burnout	6.2	2.0
FFM Flight Mode (Backup)	9.0	
Black Brant Ignition	12.0	5.0
Black Brant Burnout	44.4	42.2
Nosecone eject	68.0	85.7
2 nd -3 rd Stage Separation	72.0	92.6
Nihka Ignition	76.0	99.3
Nihka Burnout	94.6	148.0
FFM Reset (Time synch)	100.0	168.2
FFM Release	137.0	301.1
Despin	150.0	
1 st FFM Transmission	400.0	
2 nd FFM Transmission	700.0	
3 rd FFM Transmission	1000	
Ballistic Impact	1132	0.0

Table-2 FFM Mission Events

released the FFMs spun up to ~17 Hz and left the rocket with a relative velocity of ~3 m/s.

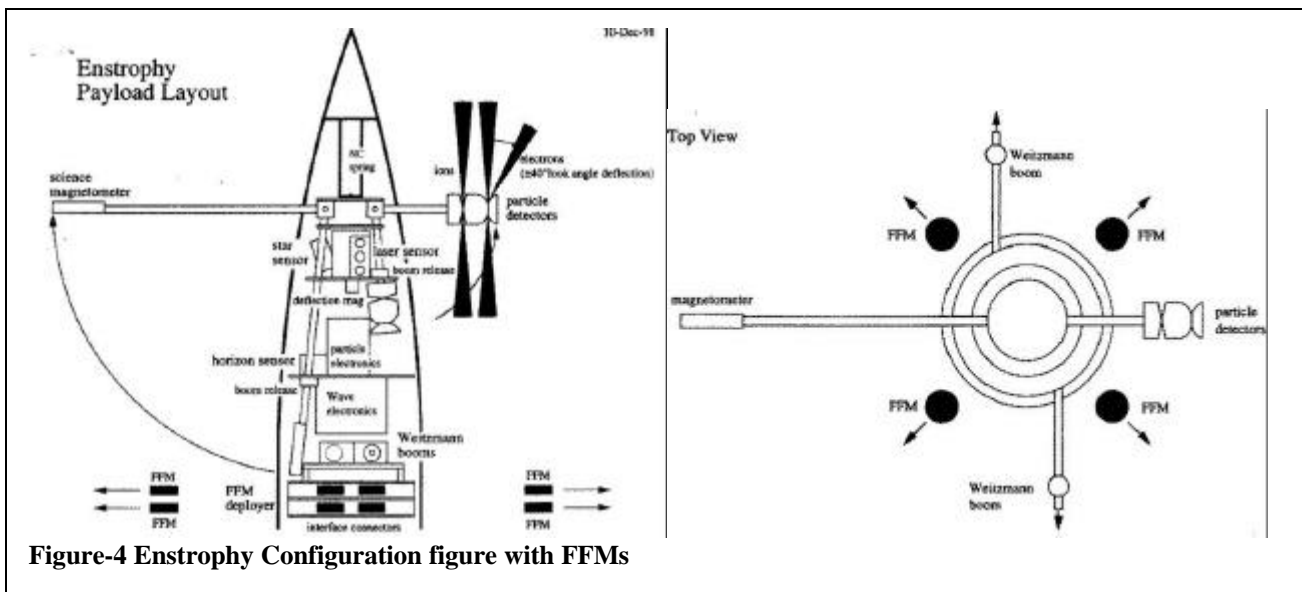


Figure-4 Enstrophy Configuration figure with FFMs

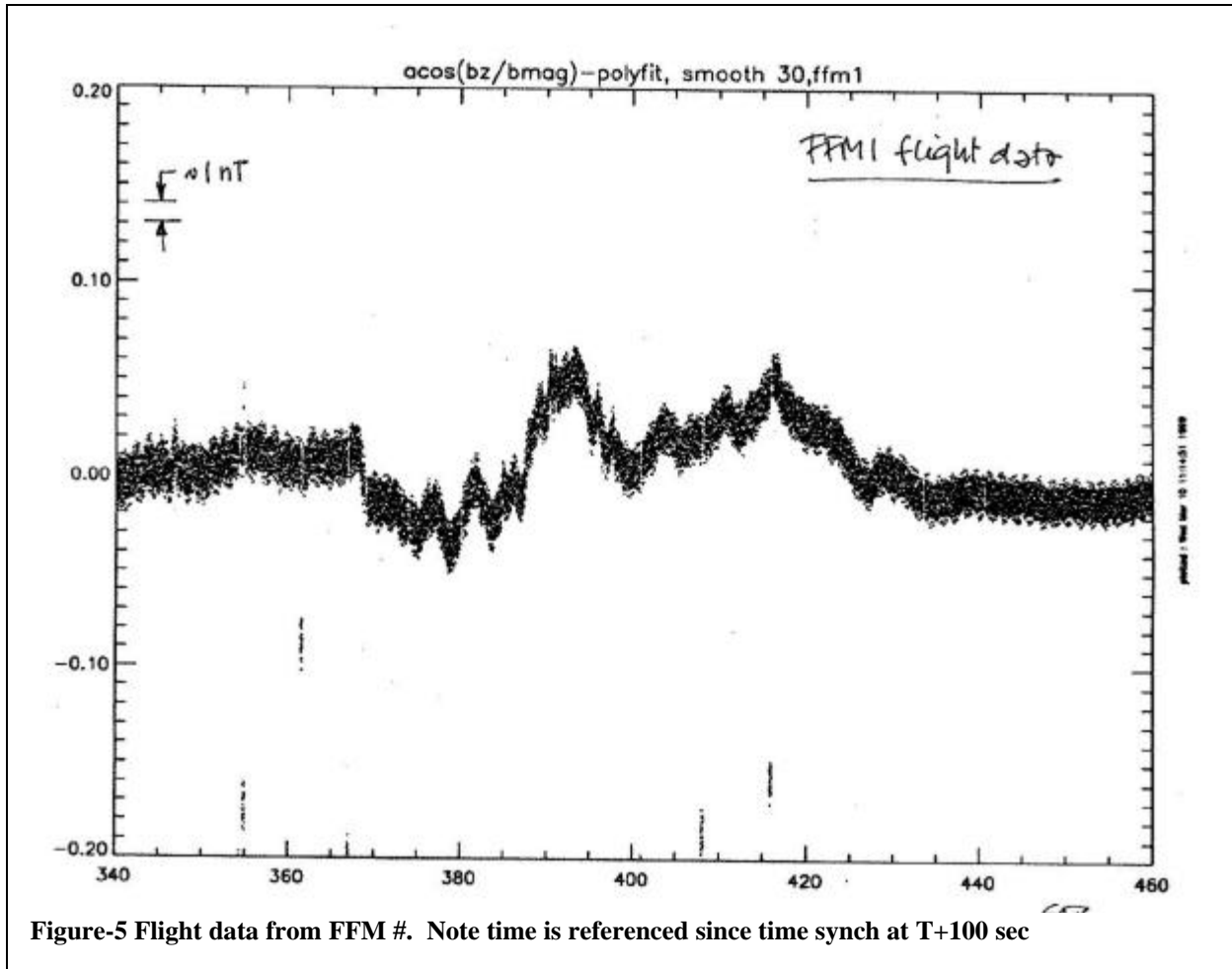


Figure-5 Flight data from FFM #. Note time is referenced since time synch at T+100 sec

The FFMs began taking data once the time synch pulse ("reset") was received. Five minutes after the FFMs received the synch pulse the FFMs downlinked the data to the Poker Flats ground station. This cycle of data collection/ transmission was repeated every 5 minutes throughout the flight.

Data was received from all four FFMs during the first transmission. During the second and third transmissions data from 3 three of the FFMs were received. The fourth FFM had lower than nominal signal strength and the Poker Flats Ground system was unable to lock on to receive the data. JPL is currently working with the raw data to see if the final 2 transmissions can be salvaged.

Figure-5 shows a graph of the magnetometer data from one of the FFMs. This graph shows the passage of the FFM through an auroral arc.

CONCLUSION

The successful flight of the FFMs has validated that the sensorcraft concept can be applied to a scientific problem. In addition to demonstrating the sensorcraft concept the



Figure-6 FFM Family Portrait

FFMs demonstrated several key technologies that will be required for future applications of this concept.

Currently there are studies under way exploring the future use of a 2nd generation of FFM like sensor crafts.

ACKNOWLEDGEMENTS

A portion of this work was performed by the Center for Space Microelectronics Technology, Jet Propulsion Laboratory, California Institute of Technology, and was sponsored by the National Aeronautics and Space Administration. We also like to thank D. Hepner (USARL, Aberdeen Proving Ground); C. Cruzan, E. Cutting, S. DiStefano, J. Burpo, C. Greenhall, T. McCann, J. Rademacher, B. Thoma, D. Wallace (JPL); M. Widholm (University of New Hampshire); T. Stirling, C. Lankford (NASA Wallops); and the Enstrophy integration team at Poker Flat, Alaska for their support.

REFERENCES

[1] R. Goldstein, M. Boehm, K.A. Lynch, H. Javadi, R.A. Wallace, "Autonomous, Free-Flying Nano-Spacecraft Fleets for Space Physics Measurements", *To be presented in the American Geophysical Union 1999 Spring Meeting, Special Session on New Missions*.

[2] K.A. Lynch, Y. Zheng, R. Arnoldy, M. Boehm, R. Goldstein, H. Javadi, P. Kintner, P. Schuck, E. Klatt, H. Stenbaek-Nielsen, T. Hallinan, L. Peticolas, "Multiple Free-Flyer Magnetometer Measurements of Auroral Electric Currents: Results from the Enstrophy Sounding Rocket Mission", *American Geophysical Union 1999 Spring Meeting*.

[3] M. Boehm, Y. Zheng, K.A. Lynch, R. Goldstein, H. Javadi, "Analysis of Enstrophy Sounding Rocket Free-Flyer Magnetometer Data: Techniques, Accuracy, and Results", *American Geophysical Union 1999 Spring Meeting*.

[4] H. Javadi, et. all, "First-Generation Jet Propulsion Laboratory "Hockey-Puck" Free-Flying Magnetometers for Distributed In-Situ Multiprobe Measurement of Current Density Filamentation in the Northern Auroral Zone: Enstrophy Mission", *Micro-nano Technology Conference, April 11-15, 1999*

[5] Cardinal Components, Inc., 155 Route 46 West, Wayne, New Jersey 07470.

[6] MicroPulse, Inc., 409 Calle San Pablo, Camarillo, CA 93012.

[7] Eagle Picher Industries, Inc., C&Porter Streets, Joplin, MO 64804.

[8] US Army Research Laboratory, Aberdeen Proving Ground, MD 21005

